

Supporting Information

Stretchable, sensitive, flexible strain sensor incorporated with patterned liquid metal on hydrogel for human motion monitoring and human-machine interaction

Huaping Wu ^{a,b}, Hangcheng Qi ^{a,b}, Xueer Wang ^c, Ye Qiu ^{a,b}, Kuanqiang Shi ^{a,b}, Hengjie Zhang ^{a,b}, Zheng Zhang ^{a,b}, Wenan Zhang ^{c,*} and Ye Tian ^{a,b,*}

^a College of Mechanical Engineering, Zhejiang University of Technology, Hangzhou, 310023, China;

^b Key Laboratory of Special Purpose Equipment and Advanced Processing Technology, Ministry of Education and Zhejiang Province, Zhejiang University of Technology, Hangzhou, 310023, China

^c College of Information Engineering, Zhejiang University of Technology, Hangzhou, 310023, China

Corresponding Author

Wenan Zhang, Email: wazhang@zjut.edu.cn

Ye Tian, Email: tianye@zjut.edu.cn

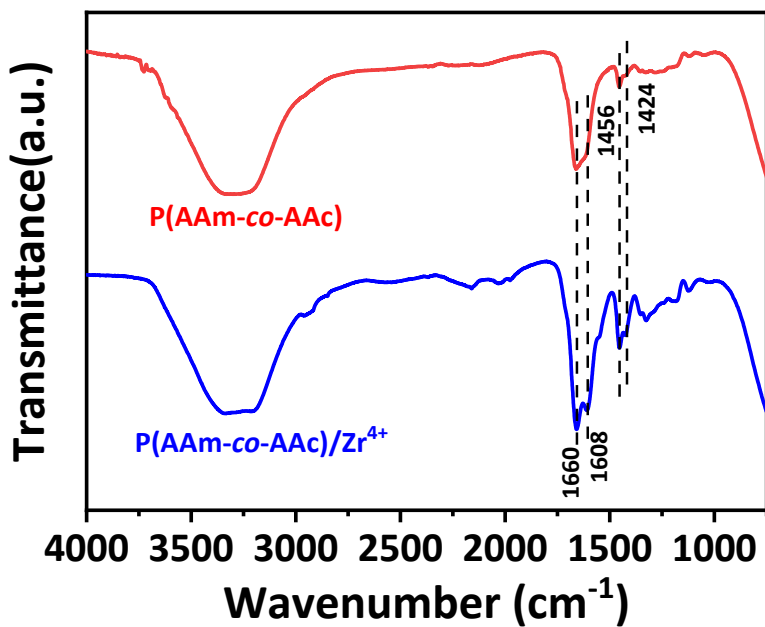


Figure S1. FTIR spectra of equilibrated P(AAm-*co*-AAc) ($C_m = 5 \text{ M}$, $f_{\text{AAc}} = 30 \text{ mol\%}$) and P(AAm-*co*-AAc)/ Zr^{4+} ($C_m = 5 \text{ M}$, $f_{\text{AAc}} = 30 \text{ mol\%}$, $C_{\text{Zr}^{4+}} = 0.5 \text{ M}$) hydrogel films.

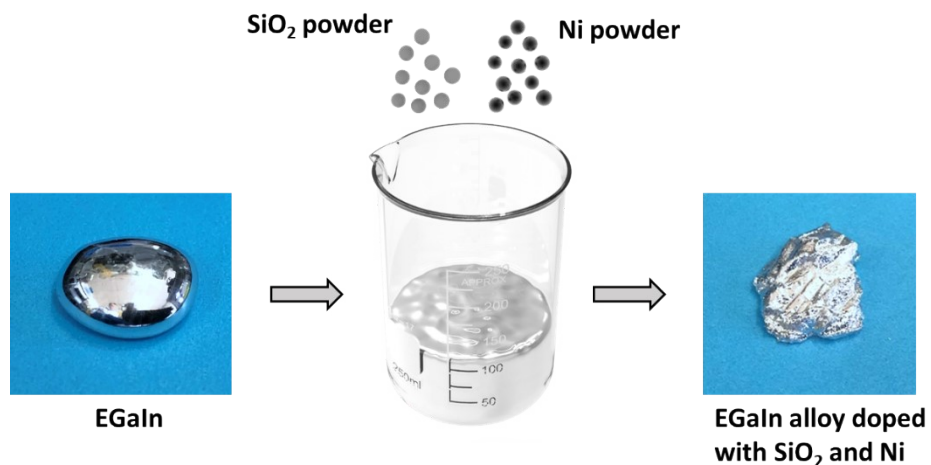


Figure S2. Schematic diagram of the preparation of EGaIn alloy doped with SiO_2 and Ni.

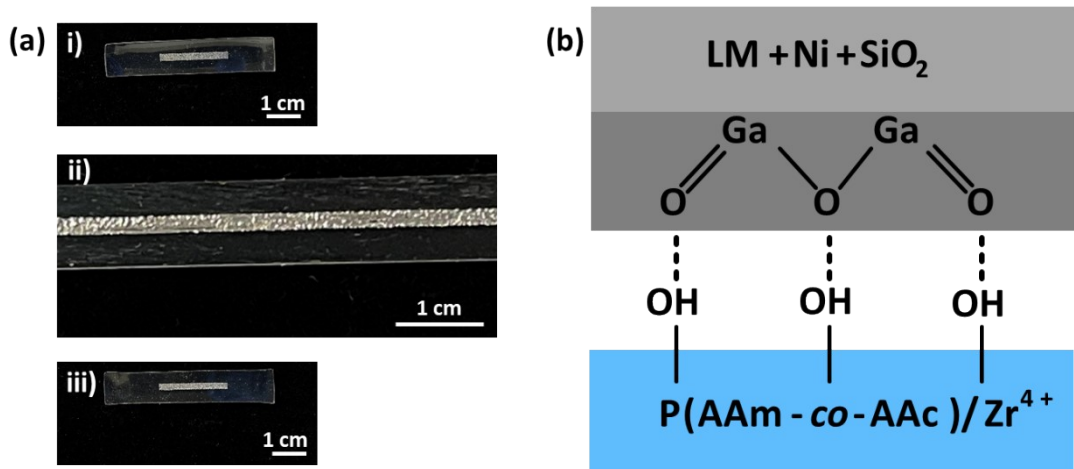


Figure S3. (a) Photographs of linear LM strip shadow printed on the hydrogel surface (i) before, (ii) after applying a tensile strain of 300% and (iii) after recovery from stretching for 300 times. (b) Schematic diagram of interfacial adhesion between the LM and hydrogel layers.

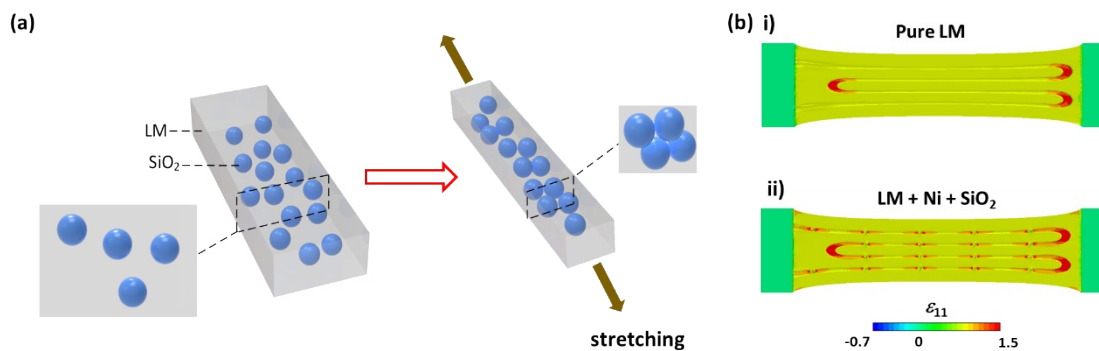


Figure S4. (a) Diagram of LM doped with SiO_2 particles before and after stretching. (b) Finite element analysis of tensile strain of the strain sensor patterned with (i) pure LM and (ii) LM doped with Ni and SiO_2 particles.

Table S1. Comparison of the maximum gauge factor and strain of flexible strain

sensors.

Materials	Strain (%)	Gauge factor	Reference ^a
LM/P(AAm- <i>co</i> -MAAc)	630	1.42	S1
LM/Ecoflex	396	2.20	S2
LM/PVA	375	0.73	S3
oxCNTs/PAAm	700	3.39	S4
PANI/P(AAm- <i>co</i> -HEMA)	300	1.48	S5
AgNPs/PDMS	70	10.80	S6
CB/PDMS	30	0.20	S7
MWCNTs/PDMS	40	7.22	S8
CB/CNT/TPU	50	4.10	S9
PEDOT:SL/PAAc	100	7.00	S10

References^a

- S1 X. P. Hao, C. Y. Li, C. W. Zhang, M. Du, Z. Ying, Q. Zheng and Z. L. Wu, *Adv. Funct. Mater.*, 2021, 2105481.
- S2 Y. Mengucci, Y.-L. Park, H. Pei, D. Vogt, P. M. Aubin, E. Winchell, L. Fluke, L. Stirling, R. J. Wood and C. J. Walsh, *Int. J. Rob. Res.*, 2014, 33, 1748–1764.
- S3 C. Xu, B. Ma, S. Yuan, C. Zhao and H. Liu, *Adv. Electron. Mater.*, 2020, 6, 1900721.
- S4 X. Sun, Z. Qin, L. Ye, H. Zhang, Q. Yu, X. Wu, J. Li and F. Yao, *Chem. Eng. J.*, 2020, 382, 122832.
- S5 Z. Wang, J. Chen, Y. Cong, H. Zhang, T. Xu, L. Nie and J. Fu, *Chem. Mater.*, 2018,

30, 8062–8069.

S6 H. M. Soe, A. A. Manaf, A. Matsuda and M. Jaafar, *J. Mater. Sci.: Mater. Electron.*, 2020, 31, 11897–11910.

S7 X. Cheng, C. Bao, X. Wang and W. Dong, *Proc. Inst. Mech. Eng., Part L: J. Mater.: Des. Appl.*, 2020, 234, 496–503.

S8 T. Li, J. Li, A. Zhong, F. Han, R. Sun, C.-P. Wong, F. Niu, G. Zhang and Y. Jin, *Sens. Actuators A*, 2020, 306, 111959.

S9 M. Go, X. Qi, P. Matteini, B. Hwang and S. Lim, *Sens. Actuators A*, 2021, 332, 113098.

S10 Q. Wang, X. Pan, C. Lin, D. Lin, Y. Ni, L. Chen, L. Huan, S. Cao and X. Ma, *Chem. Eng. J.*, 2019, 370, 1039–1047.

Table S2. Comparison of the detection limit and sensing range of flexible strain sensors.

Materials	Sensing range (%)	Detection limit	Reference^b
			(%)
Ag/rGO/PDMS	200	0.20	S11
MXene/PANIF/VHB	80	0.15	S12
CS/MWCNT/PDMS	80	0.40	S13
LM/Ecoflex	310	0.09	S14
PANI/P(AAm- <i>co</i> -HEMA)	300	0.30	S15
CB/TPU/Ecoflex	225	0.50	S16
Ag/MWCNT/G/PDMS	170	0.10	S17
PAAm/Carrageenan	400	0.50	S18
CNT/TPU	600	0.05	S19
CNT/PDMS	100	0.01	S20

References^b

S11 L. Zhang, H. Kou, Q. Tan, G. Liu, W. Zhang and J. Xiong, *J. Phys. D: Appl. Phys.*, 2019, 52, 395401.

S12 M. Chao, Y. Wang, D. M, X. W, W. Zhang, L. Zhang and P. Wan, *Nano Energy*, 2020, 78, 105187.

S13 B. Zhang, W. Wang, D. Zhang, T. Li, H. Zhang, C. Du, W. Zhao and Y. Yang, *J. Mater. Chem. C*, 2021, 9, 14848–14857.

S14 J. Chen, J. Zhang, Z. Luo, J. Zhang, L. Li, Y. Su, X. Gao, Y. Li, W. Tang, C. Cao,

- Q. Liu, L. Wang and H. Li, *ACS Appl. Mater. Interfaces*, 2020, 12, 22200–22211.
- S15 Z. Wang, J. Chen, Y. Cong, H. Zhang, T. Xu, L. Nie and J. Fu, *Chem. Mater.*, 2018, 30, 8062–8069.
- S16 Y. Zhao, M. Ren, Y. Shang, J. Li, S. Wang, W. Zhai, G. Zheng, K. Dai, C. Liu and C. Shen, *Compos. Sci. Technol.*, 2020, 200, 108448.
- S17 J. Lin, X. Cai, Z. Liu, N. Liu, M. Xie, B. Zhou, H. Wang and Z. Guo, *Adv. Funct. Mater.*, 2020, 30, 2000398.
- S18 J. Wu, Z. Wu, X. Lu, S. Han, B.-R. Yang, X. Gui, K. Tao, J. Miao and C. Liu, *ACS Appl. Mater. Interfaces*, 2019, 11, 9405–9414.
- S19 H. Li, J. Chen, X. Chang, Y. Xu, G. Zhao, Y. Zhu and Y. Li, *J. Mater. Chem. A*, 2021, 9, 1795–1802.
- S20 J. Chen, G. Zhu, F. Wang, Y. Xu, C. Wang, Y. Zhu and W. Jiang, *Compos. Sci. Technol.*, 2021, 213, 108932.

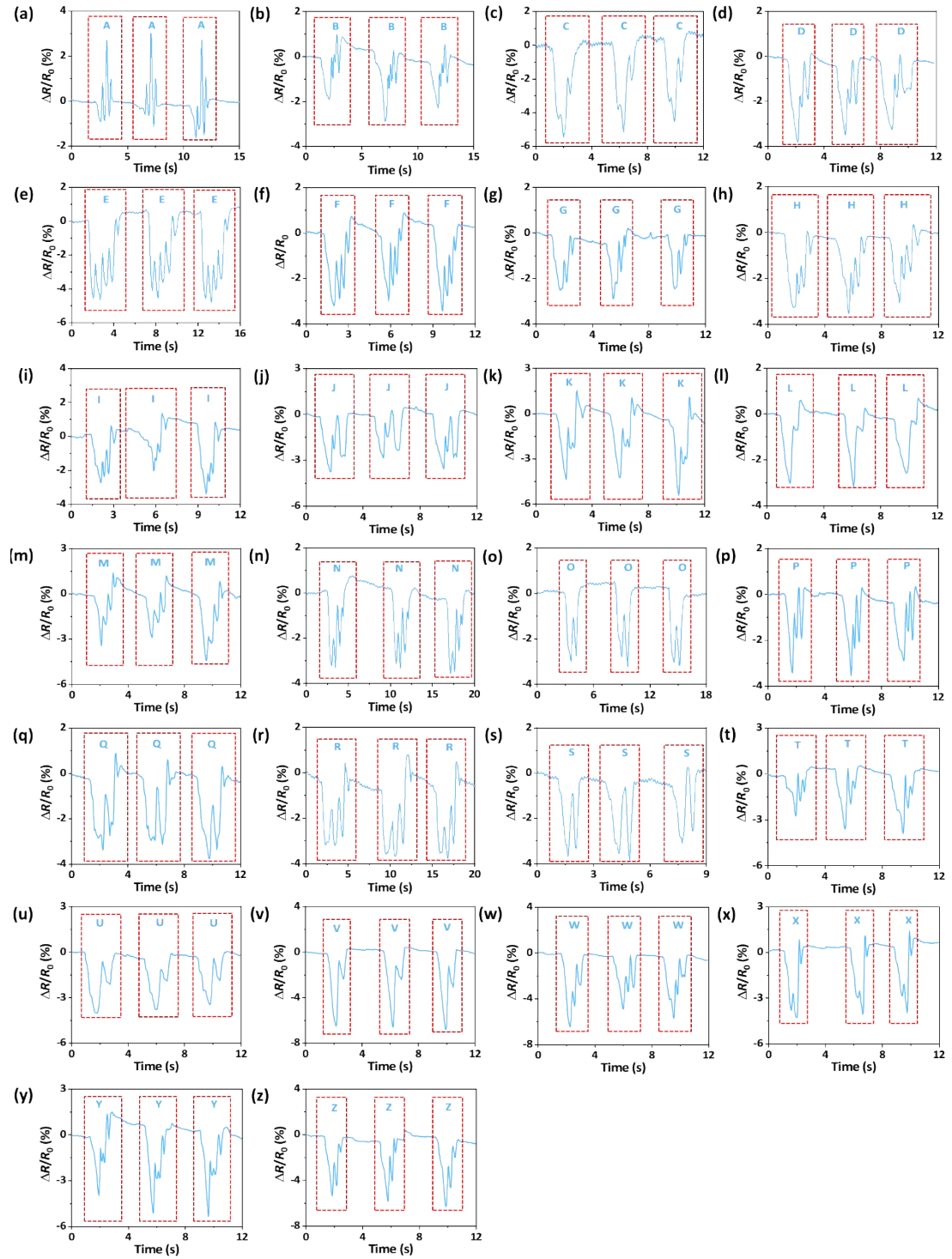


Figure S5. The relative resistance change curves for detection of handwriting different letters.

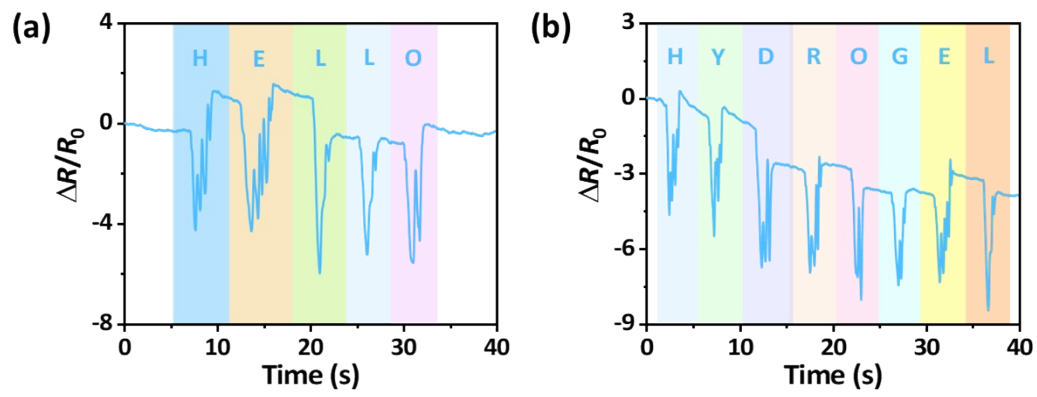


Figure S6. The relative resistance change curves for detection of handwriting different words, (a) "HELLO", and (b) "HYDROGEL".